



High apparent adhesion energy in the breakdown of normal restitution for binary impacts of small spheres at low speed

C.M. Sorace, M.Y. Louge*, M.D. Crozier, V.H.C. Law

Sibley School of Mechanical and Aerospace Engineering, Cornell University, 192 Rhodes Hall, Ithaca, NY 14850, USA

ARTICLE INFO

Article history:

Received 14 August 2008

Available online 5 November 2008

PACS:

45.50.Tn

46.55.+d

68.35.Np

68.35.Md

Keywords:

Impact

Adhesion

Restitution

ABSTRACT

We measure kinematic coefficients of normal restitution in head-on collisions of two identical small spheres of acrylic, ceramic or steel suspended by thin resilient strands at low enough impact speeds for adhesion to lower the restitution. We observe such reduction at speeds consistent with an apparent adhesion surface energy larger than expected.

© 2008 Elsevier Ltd. All rights reserved.

1. Introduction

The behavior of two colliding grains ultimately governs the dynamics of granular gases engaged in binary impacts. Although the collisions of two solids of arbitrary shape is not in general described by kinematics alone (Stronge, 2000; Smith and Liu, 1992), theories for ideal granular gases often assume that head-on impacts of two relatively hard spheres have a single point of contact and possess a kinematic coefficient of normal restitution e such that

$$\mathbf{v}^- \cdot \hat{\mathbf{n}} = -e \mathbf{v}^+ \cdot \hat{\mathbf{n}}, \quad (1)$$

where $\mathbf{v} = \mathbf{c}_1 - \mathbf{c}_2$ is the relative velocity of spheres 1 and 2, \mathbf{c} is their absolute velocity, $\hat{\mathbf{n}}$ is the unit vector joining their centers, and the superscripts + and – denote quantities immediately before and after impact.

While most granular theories (Lun et al., 1984; Jenkins and Richman, 1985; Sela and Goldhirsch, 1998; Montanero et al., 1999) assume constant normal restitution, Turner and Woodcock (1990), Weber et al. (2004), Rognon et al. (2008), Brewster et al. (2005) and McNamara and Falcon (2008) have recognized how collective grain dynamics is affected by reductions in e due to material failure (Lifshitz and Kolsky, 1964; Vu-Quoc et al., 2000) or visco-elastic energy loss (Ramírez et al., 1999) in rapid impacts.

Van der Waals attraction also reduces normal restitution at low collision speed. In that regime, the contact adhesion theories of elastic (Johnson et al., 1971; Derjaguin et al., 1975; Maugis, 1992), elasto-plastic (Thornton and Ning, 1998;

* Corresponding author. Tel.: +1 607 255 4193; fax: +1 607 255 1222.

E-mail address: MYL3@cornell.edu (M.Y. Louge).

Mesarovic and Johnson, 2000), and visco-elastic (Attard, 2001; Haiat et al., 2003; Brilliantov et al., 2007) spheres reassure theorists of granular gas dynamics that, at the relatively low surface energies of typical grain materials, adhesion should make e vanish only for particles of very small size at low impact speed. Nonetheless, in this paper, we offer experimental evidence that normal restitution for spheres as large as a few mm can breakdown at impact velocities higher than hitherto expected. In other words, for inelastic collisions, apparent surface energies seem to be larger than equilibrium values for the same contacting solids.

This phenomenon eluded earlier observations, perhaps because sphere diameters or impact speeds were larger than our own. Conventional wisdom is that $e \lesssim 1$ at $v^+ = 0$, and that e continuously decreases as $v^+ \equiv |\mathbf{v}^+ \cdot \hat{\mathbf{n}}|$ grows. This is the behavior that Hatzes et al. (1988) and Supulver et al. (1995) reported with ice spheres of 4–40 cm diameter. Using pendula holding 25 mm steel spheres, Stevens and Hrenya (2005) also found e rolling off at large v^+ , and interpreted observations with available theories. Labous et al. (1997) did so for their 6–25 mm binary collisions of nylon spheres.

Evidence of the breakdown of e at low speeds is limited. By repeatedly bouncing an 8 mm diameter carbide sphere off a plate, Falcon et al. (1998) reported decreasing restitution as the contact duration eventually caught up with the ballistic time of flight between two consecutive impacts. Interestingly, the raw data of Supulver et al. (1995) with a rubber ball or Hatzes et al. (1988) with ice spheres also hint at the existence of a roll-off toward low speeds, $e \rightarrow 0$ as $v^+ \rightarrow 0$. Quinn (2005) observed such roll-off for impacts of a convex object on a plate at low v^+ , and attributed this to the external force that he superimposed on the colliding solids. For isolated impacts at low speed, Thornton and Ning (1998), Mesarovic and Johnson (2000) and Brilliantov et al. (2007) identified this force as adhesion.

2. Apparatus

Fig. 1 sketches the pendular collision apparatus. Two identical, small spheres of material density ρ , diameter d , Young modulus E , Poisson ratio ν , van der Waals surface energy γ and mass $m = \rho(\pi/6)d^3$ are attached by a single dab of cyanoacrylate adhesive to two strands of Honeywell Spectra 9000, diameter 9 μm , forming a V with apex angle $\approx 30^\circ$ and constraining the spheres to swing on circular trajectories of radius $R \approx 100$ mm. (Spectra has the highest strength/weight ratio of any fiber, so is an ideal support of negligible mass. Other strand material such as human hair, copper wire, or dental floss do not keep taut while holding relatively light spheres).

The four silk strands are carefully adjusted to equal length using guitar tuners, so the resulting pendula are constrained to rotate along the same axis with unit vector $\hat{\mathbf{y}}$. The suspension assembly of one of the spheres is moved to the correct location using fine translation stages along three cartesian axes aligned with the unit vectors $\hat{\mathbf{y}}$, $\hat{\mathbf{n}}$, and the unit vertical $\hat{\mathbf{z}}$ directed against the gravitational acceleration \mathbf{g} . At rest, the suspension axes of the two pendula are directed along $\hat{\mathbf{z}}$, while the spheres just touch with line of centers along $\hat{\mathbf{n}} = \hat{\mathbf{y}} \times \hat{\mathbf{z}}$.

To adjust their lengths while providing sharp corners around which they will later describe half-swings without slip between impacts, the relatively fragile strands are wrapped along shallow grooves cut on hemi-cylindrical blocks. A symmet-

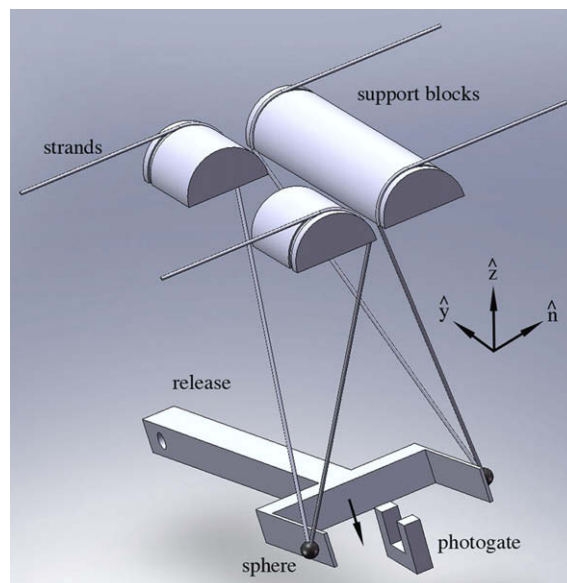


Fig. 1. Sketch of the pendular apparatus. Each sphere is suspended by a V-shaped strand held in place by grooves cut in support blocks. Spheres are released by quickly rotating the bottom mechanism in the direction shown and describe successive half-swings between impacts. They move freely through the gap of the photogate. The guitar tuners, the micrometer assembly that adjusts the position of the wide block, and the camera are not shown. For clarity, vectors of the coordinate axes are sketched away from the origin at the spheres' contact point, and sphere and strand sizes are exaggerated.

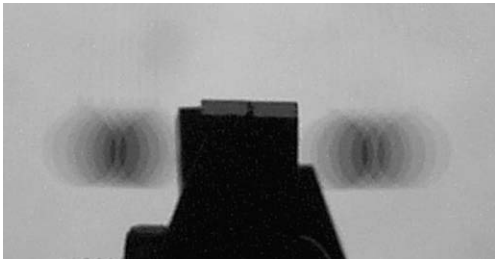


Fig. 2. A typical stroboscopic photograph of successive apogees for small-amplitude, low-velocity swings of acrylic spheres. The dark outline of the photogate is visible in the foreground.

rical mechanism actuated by a solenoid releases both spheres simultaneously without appreciable spin. To ensure that the center of mass of the combined two-sphere system does not swing away from the vertical axis, two arms separate the spheres equally from the impact site and release them from the same height.

Stroboscopic photographs are recorded by a Kodak DC 290 digital camera with 1792×1200 pixels, on an optical axis along \hat{y} , at a 6 s exposure, producing highly contrasted sphere outlines against diffuse backlighting (Fig. 2). Lenses produce close-up photographs with resolution equivalent to 150–550 pixels/cm with negligible distortion, allowing observations of narrow or wide swing amplitudes corresponding to low or high velocity impacts, respectively. A focusing target made of an array of cartesian lines and circles calibrates the image size, verifies the absence of distortion or parallax, checks that sphere

Table 1
Sphere properties: d (mm), ρ (g/cm³), E (GPa), and ν . Parameters fitted to Thornton and Ning (1998): σ_Y (GPa), γ_a^T (J/m²). Parameters fitted to Brilliantov et al. (2007): A (μ s), γ_a^B (J/m²). Restitution e_∞ observed at high speed.

Material	d	ρ	E	ν	σ_Y	γ_a^T	A	γ_a^B	e_∞
Ceramic	3	3.86	370	.26	3.9	100	0.024	92	$0.95_8 \pm 0.05$
Steel	3	7.92	190	.28	1.8	56	0.19	45	$0.90_4 \pm 0.04$
Acrylic	3.96	1.22	3	0.35	0.073	22	0.44	14	$0.91_8 \pm 0.05$

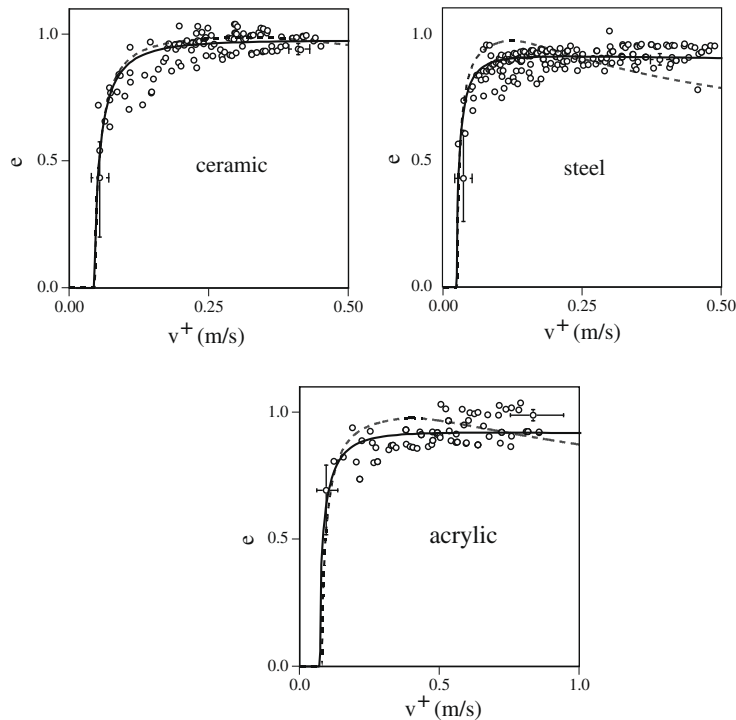


Fig. 3. Normal restitution e for ceramic, steel, and acrylic spheres versus relative speed v^+ before impact. Symbols are data points; for clarity, typical error bars are only shown at one low speed and one high speed; dashed and solid lines are, respectively, least-squares fit to the elasto-plastic theory of (Thornton and Ning, 1998) and the visco-elastic theory of (Brilliantov et al., 2007).

centers reside on the object plane, and fixes the origin of $(\hat{\mathbf{n}}, \hat{\mathbf{y}}, \hat{\mathbf{z}})$ at the point of contact. Wider photographs viewing both spheres and their pendular pivot points are used to check alignment accuracy and to determine R .

A photogate consisting of an infrared light-emitting diode and a detector positioned on opposite sides of the particle path records when spheres reach perigee. For each swing, a computer acquires the photogate pulse, updates the pendulum period, predicts when spheres reach their apogee, and triggers the stroboscopic flash at that instant. Because spheres have vanishing velocity at apogee, small errors in the timing of the flash are inconsequential. Photographs are analyzed by overlaying a circle on sphere outlines using commercial photo-editing software. For best accuracy, the vertical elevations z_i of successive sphere centers at apogee are calculated from their horizontal coordinates n_i using $z_i = R - \sqrt{R^2 - n_i^2}$. From this, we infer the total energy $\mathcal{E}_i = mgz_i$ of each sphere as it passes through its i -th apogee on the side of its hemi-cylindrical block.

Impact experiments are preceded by calibrations in which each sphere moves alone in a series of progressively shorter full swings. Such tests allow us to model the energy dissipation possibly induced by drag on the pendulum and friction in the strands, and to check that each sphere describes a circular trajectory in the half-swing on the side of its supporting block. The total energy at the end of a swing is proportional to that at its onset, $\mathcal{E}_{i+1} = (1 - \epsilon)\mathcal{E}_i$ with $\epsilon \ll 1$, indicating that the fractional energy dissipation ϵ in a full swing is proportional to total energy. This suggests that losses arise from the work of viscous or frictional forces that are proportional to the instantaneous velocity of the pendulum. Using this information, we calculate the relative velocities before and after impact from

$$|\mathbf{v}^\pm \cdot \hat{\mathbf{n}}| = \sqrt{2gz_1^\pm \left(1 \mp \frac{\epsilon}{4}\right)} + \sqrt{2gz_2^\pm \left(1 \mp \frac{\epsilon}{4}\right)}, \quad (2)$$

where velocities just before and after contact are calculated, respectively, from the preceding (superscript +) and following (superscript −) elevations z_1 and z_2 of the two apogees corrected for total energy loss in a quarter swing. We then deduce e from Eq. (1).

The apparatus produced impacts of alumina ceramic, acrylic and 302-stainless steel spheres with properties summarized in Table 1. To verify that electrostatics played a negligible role, we reproduced experiments near a 150 mm-wide EXAIR “Ionizing bar” connected to a 5 kV power supply. By creating an equal number of positive and negative charges in the surrounding air, the bar neutralized static electricity that may have accumulated on the spheres and supporting apparatus. By repeating experiments in summer and winter, we also gauged effects of relative humidity in the range 14–51%. Because we could discern no change in the variations of e versus v^+ , neither electrostatic nor capillarity forces played a role in the results. Finally, because results were insensitive to the heights at which spheres were originally released, or to how many times they had previously bumped, successive collisions did not affect e , unlike the more violent impacts of Falcon et al. (1998) and Weir and Tallon (2005) that involved relatively massive spheres.

3. Results

Fig. 3 shows experimental data. Restitution at large speed agrees with the free-fall binary impact results of Lorenz et al. (1997) and Louge et al. (2000). To within experimental error, e clearly rolls off at low impact speeds. Dashed lines mark the least-squares fit of e versus v^+ to the apparent surface energy γ_a^T and yield strength σ_Y of the elasto-plastic theory of Thornton and Ning (1998), which these authors reported in closed-form.¹ The resulting yield strength is reasonable for our materials. Solid lines are least-squares fits to the apparent surface energy γ_a^B and relaxation time A of the visco-elastic theory of Brilliantov et al. (2007).² Although the two theories differ in their predictions of e versus v^+ , their values of γ_a^B and γ_a^T found in Table 1 are consistent, but much larger than equilibrium surface energies, which we expected to be on the order of $\gamma \sim 0.4\text{--}4\text{ J/m}^2$ for metals (Tewary and Fuller, 1990; Israelachvili, 1992), $\gamma \simeq 1.6\text{--}11\text{ J/m}^2$ for alumina ceramic (Siegel et al., 2003) and $\gamma \simeq 0.04\text{ J/m}^2$ for plastics (Lee, 1991).

A tempting explanation is that another quantity is involved. For example, Maugis (1992) introduced a parameter λ reconciling the theories of Johnson et al. (1971) (JKR; $\lambda \rightarrow \infty$) and Derjaguin et al. (1975) (DMT; $\lambda \rightarrow 0$) for elastic adhesive spheres. Our numerical integration of his equations of motion yields a critical velocity at which e vanishes,

$$v_{\text{crit}}^+ = \sqrt{\frac{6C(\lambda)}{\pi} \frac{\gamma^{5/3}(1 - v^2)^{2/3}}{\rho d^{5/3} E^{2/3}}}, \quad (3)$$

similar to Eq. (54) of Thornton and Ning (1998), where $C_\infty \equiv C(\lambda \rightarrow \infty) \simeq 7.0921_9$ and $C(\lambda = 0) = 0$ in the JKR and DMT limits, respectively, and $C(\lambda) \simeq \lambda(C_\infty \lambda^3 - 3.6\lambda^2 + 5\lambda + 0.14)/(\lambda^4 - 0.49\lambda^3 + 0.47\lambda^2 + 0.079\lambda + 0.00036)$ is a fit for other values of λ . Because $C(\lambda) < \max(C) \simeq 8.5362_1$ with $\max(C) > C_\infty$, and because $\gamma \propto 1/C^{3/5}$ at a given v_{crit}^+ , the apparent surface energy inferred from our experiments could be smaller than in Table 1, if we adopted a finite $\lambda \sim 0.68$ instead of the Johnson et al. (1971) limit. However, because γ_a would merely be reduced by $<1 - (C_\infty/C_{\text{max}})^{3/5} \simeq 11\%$, such reduction could not explain why we recorded high apparent surface energies. Greenwood (1997) proposed an alternative elastic theory, with similarly negligible effects on γ_a . Therefore, reasons for high γ_a must be found elsewhere.

¹ Equation (81) of Thornton and Ning (1998) contains a typo. The leading constant should read $6\sqrt{3}/5$.

² For consistency with Johnson et al. (1971), we integrate the equation of motion (33) of Brilliantov et al. (2007) until the contact radius $a_{\text{sep}} = [(\pi/6)\gamma DR_{\text{eff}}^2]^{1/3}$ and force $F_{\text{sep}} = -(5\pi/6)\gamma/R_{\text{eff}}$, rather than to the a_{sep} and F_{sep} that Brilliantov et al. (2007) assumed in their Eqs. (15) and (16).

In that quest, it is instructive to recall the hysteretic behavior of energy between loading and unloading of solid–solid contacts in polymers (Chaudhury and Whitesides, 1991, 1992; Chaudhury and Owen, 1993; Chaudhury et al., 1996). Such hysteresis, which involves higher surface energies upon unloading (Zeng et al., 2006; Alcantar et al., 2003), may be related to our anomalously high apparent adhesion energies. For metals, Brenner et al. (1981) and Veistinen and Lindroos (1984) also reported apparent surface energies above equilibrium values (Rogers and Reed, 1984), suggesting that unloading requires work closer to that for crack propagation (Cook, 1986; Tattersall and Tappin, 1966). In other words, it seems as though inelastic impacts fuse material locally in the loading phase, perhaps at surface asperities, thus requiring higher work for unloading and separation. In turn, this might produce the breakdown of normal restitution at critical velocities higher than expected.

Acknowledgements

The authors are grateful to N. Brilliantov, S. Daniel, C.-Y. Hui, J. Israelachvili, S. Mesarovic, A. Valance and H. Xu for fruitful conversations, and to M. Egan, C. J. Fontana, E. Franjul, D. Grubb, S. Keast, J. Kwak, A. Lapsa, E. Palermo, D. Tagatac and P. Weisz for help with experiments. This work was supported by NASA grant NAG3-2705.

References

- Alcantar, N.A., Park, C., Pan, J.-M., Israelachvili, J.N., 2003. Adhesion and coalescence of ductile metal surfaces and nanoparticles. *Acta Mater.* 51, 31–47.
- Attard, P., 2001. Interaction and deformation of viscoelastic particles. 2. Adhesive particles. *Langmuir* 17, 4322–4328.
- Brenner, S.S., Wriedt, H.A., Oriani, R.A., 1981. Impact adhesion of iron at elevated temperatures. *Wear* 68, 169–190.
- Brewster, R., Grest, G.S., Landry, J.W., Levine, A.J., 2005. Plug flow and the breakdown of Bagnold scaling in cohesive granular flows. *Phys. Rev. E* 72, 061301.
- Brilliantov, N.V., Albers, N., Spahn, F., Pöschel, T., 2007. Collision dynamics of granular particles with adhesion. *Phys. Rev. E* 76, 051302.
- Chaudhury, M.K., Owen, M.J., 1993. Correlation between adhesion hysteresis and phase state of monolayer films. *J. Phys. Chem.* 97, 5722–5726.
- Chaudhury, M.K., Weaver, T., Hui, C.-Y., Kramer, E.J., 1996. Adhesive contact of cylindrical lens and a flat sheet. *J. Appl. Phys.* 80, 30–37.
- Chaudhury, M.K., Whitesides, G.M., 1991. Direct measurement of interfacial interactions between semispherical lenses and flat sheets of poly(dimethylsiloxane) and their chemical derivatives. *Langmuir* 7, 1013–1025.
- Chaudhury, M.K., Whitesides, G.M., 1992. Correlation between surface free energy and surface constitution. *Science* 255, 1230–1232.
- Cook, R.F., 1986. Crack propagation thresholds: a measure of surface energy. *J. Mater. Res.* 1, 852–860.
- Derjaguin, B., Muller, V., Toporov, Y.P., 1975. Effect of contact deformations on the adhesion of particles. *J. Colloid Interf. Sci.* 53, 314–326.
- Falcon, E., Laroche, C., Fauve, S., Coste, C., 1998. Behavior of one inelastic ball bouncing repeatedly off the ground. *Eur. Phys. J. B* 3, 45–57.
- Greenwood, J.A., 1997. Adhesion of elastic spheres. *Proc. R. Soc. Lond. A* 453, 1277–1297.
- Haïat, G., Huy, M.P., Barthel, E., 2003. The adhesive contact of viscoelastic spheres. *J. Mech. Phys. Solids* 51, 69–99.
- Hatzes, A.P., Bridges, F.G., Lin, D.N.C., 1988. Collisional properties of ice spheres at low impact velocities. *Mon. Not. R. Astron. Soc.* 231, 1091–1115.
- Israelachvili, J.N., 1992. *Intermolecular and Surface Forces*. Academic Press, London.
- Jenkins, J.T., Richman, M.W., 1985. Grad's 13-moment system for a dense gas of inelastic spheres. *Arch. Rat. Mech. Anal.* 87, 355–377.
- Johnson, K., Kendall, K., Roberts, A., 1971. Surface energy and the contact of elastic solids. *Proc. Roy. Soc. Lond. A* 324, 301–313.
- Labous, L., Rosato, A.D., Dave, R.N., 1997. Measurements of collisional properties of spheres using high-speed video analysis. *Phys. Rev. E* 56, 5717–5725.
- Lee, L.-H., 1991. *Fundamentals of Adhesion*. Plenum Press, New York.
- Lifshitz, J.M., Kolsky, H., 1964. Some experiments on anelastic rebound. *J. Mech. Phys. Solids* 12, 35–43.
- Lorenz, A., Tuozzolo, C., Louge, M.Y., 1997. Measurements of impact properties of small, nearly spherical particles. *Exp. Mech.* 37, 292–298.
- Louge, M., Jenkins, J., Reeves, A., Keast, S., 2000. Microgravity segregation in collisional granular shearing flows. In: Rosato, A., Blackmore, D. (Eds.), *Proceedings of the IUTAM Symposium on Segregation in Granular Material*. Kluwer Academic Publishers, Boston, MA, pp. 103–112.
- Lun, C.K.K., Savage, S.B., Jeffrey, D.J., Chepur, N., 1984. Kinetic theories for granular flow: inelastic particles in Couette flow and slightly inelastic particles in a general flowfield. *J. Fluid Mech.* 140, 223–256.
- Maugis, D., 1992. Adhesion of spheres: the JKR–DMT transition using a Dugdale model. *J. Colloid Interf. Sci.* 150, 243–269.
- McNamara, S., Falcon, E., 2008. Simulations of dense granular gases without gravity with impact-velocity-dependent restitution coefficient. *Powder Technol.* 182, 232–240.
- Mesarovic, S.D., Johnson, K., 2000. Adhesive contact of elastic–plastic spheres. *J. Mech. Phys. Solids* 48, 2009–2033.
- Montanero, J.M., Garzó, V., Santos, A., Brey, J.J., 1999. Kinetic theory of simple granular shear flows of smooth hard spheres. *J. Fluid Mech.* 389, 391–411.
- Quinn, D.D., 2005. Finite duration impacts with external forces. *ASME J. Appl. Mech.* 72, 778–784.
- Ramírez, R., Pöschel, T., Brilliantov, N.V., Schwager, T., 1999. Coefficient of restitution of colliding viscoelastic spheres. *Phys. Rev. E* 60, 4465–4472.
- Rogers, L.N., Reed, J., 1984. The adhesion of particles undergoing an elastic–plastic impact with a surface. *J. Phys. D: Appl. Phys.* 17, 677–689.
- Rognon, P.G., Roux, J.-N., Naaïm, M., Chevoir, F., 2008. Dense flows of cohesive granular materials. *J. Fluid Mech.* 596, 21–47.
- Sela, N., Goldhirsch, I., 1998. Hydrodynamic equations for rapid flows of smooth inelastic spheres, to Burnett order. *J. Fluid Mech.* 361, 41–74.
- Siegel, D.J., Hector, L.G.J., Adams, J.B., 2003. *Ab initio* study of Al–ceramic interfacial adhesion. *Phys. Rev. B* 67, 092105/1–4.
- Smith, C., Liu, P.-P., 1992. Coefficients of restitution. *ASME J. Appl. Mech.* 59, 963–969.
- Stevens, A., Hrenya, C., 2005. Comparison of soft-sphere models to measurements of collision properties during normal impacts. *Powder Technol.* 154, 99–109.
- Stronge, W.J., 2000. *Impact Mechanics*. Cambridge University Press, New York.
- Supulver, K.D., Bridges, F.G., Lin, D.N.C., 1995. The coefficient of restitution of ice particles in glancing collisions: experimental results for unfrosted surfaces. *Icarus* 113, 188–199.
- Tattersall, H.G., Tappin, G., 1966. The work of fracture and its measurement in metals, ceramics and other materials. *J. Mater. Sci.* 1, 296–301.
- Tewary, V.K., Fuller, E.R., 1990. A relation between the surface energy and the Debye temperature for cubic solids. *J. Mater. Res.* 5, 1118–1122.
- Thornton, C., Ning, Z., 1998. A theoretical model for the stick/bounce behaviour of adhesive elastic–plastic spheres. *Powder Technol.* 99, 154–162.
- Turner, M.C., Woodcock, L.V., 1990. Scaling laws for rapid granular flow. *Powder Technol.* 60, 47–60.
- Veistinen, M.K., Lindroos, V.K., 1984. Evaluation of the effective surface energy of ferrite in a 26Cr–1Mo ferritic stainless steel. *Scripta Metall.* 18, 185–188.
- Vu-Quoc, L., Zhang, X., Lesburg, L., 2000. A normal force–displacement model for contacting spheres accounting for plastic deformation: force-driven formulation. *ASME J. Appl. Mech.* 67, 363–371.
- Weber, M.W., Hoffman, D.K., Hrenya, C.M., 2004. Discrete-particle simulations of cohesive granular flow using a square-well potential. *Granular Mat.* 6, 239–254.
- Weir, G., Tallon, S., 2005. The coefficient of restitution for normal incident, low velocity particle impacts. *Chem. Eng. Sci.* 60, 3637–3647.
- Zeng, H., Maeda, N., Chen, N., Tirrell, M., Israelachvili, J., 2006. Adhesion and friction of polystyrene surfaces around T_g . *Macromolecules* 39, 2350–2363.